

Phase diagram for the exciton Mott transition in infinite-dimensional electron-hole systems

Yuh Tomio*, Tetsuo Ogawa

CREST, JST and Department of Physics, Osaka University, Toyonaka, Osaka 560-0043, Japan

Abstract

To understand the essence of the exciton Mott transition in three-dimensional electron-hole systems, the metal-insulator transition is studied for a two-band Hubbard model in infinite dimensions with interactions of electron-electron (hole-hole) repulsion U and electron-hole attraction $-U'$. By using the dynamical mean-field theory, the phase diagram in the U - U' plane is obtained (which is exact in infinite dimensions) assuming that electron-hole pairs do not condense. When both electron and hole bands are half-filled, two types of insulating states appear: the Mott-Hubbard insulator for $U > U'$ and the biexciton-like insulator for $U < U'$. Even when away from half-filling, we find the phase transition between the exciton- or biexciton-like insulator and a metallic state. This transition can be assigned to the exciton Mott transition, whereas the Mott-Hubbard transition is absent.

Key words: exciton Mott transition, electron-hole systems, two-band Hubbard model, infinite-dimensions, dynamical mean-field theory

1. Introduction

Electron-hole (e-h) systems in photoexcited semiconductors exhibit various remarkable properties depending on carrier density, temperature, etc., and have been investigated extensively both experimentally and theoretically [1]. In particular, the metal-insulator transitions have attracted interest for many years: the exciton Mott transition at high temperatures between an exciton/biexciton gas phase and an e-h plasma phase, and crossover at low temperatures between the Bose-Einstein condensation (BEC) of excitons at low density and the BCS-like condensation of e-h pairs at high density. However, the complicated tangle of the elements, two types of fermions, Coulomb interactions of both repulsion and attraction, screening effects, e-h densities, temperatures, etc., makes the physics of this

system hard to be understood. Therefore, theoretical understanding of especially the exciton Mott transition and the BEC-BCS crossover is still not sufficient.

We expect that a study from a standpoint of the strong-correlation physics provides new interpretation about the above problems. As the first step of our work, we examine the exciton Mott transition in consideration of the minimum elements, i.e., a two-band Hubbard model, by using the dynamical mean-field theory (DMFT) [2] recently developed through the study of strongly correlated electron systems. The DMFT requires only the locality of the self-energy, and can take full account of local correlations. This locality and the resulting DMFT become exact in the limit of infinite spatial dimensions and good approximation of the three-dimensional systems.

In the present paper, we focus on the normal phase where the condensation of e-h pairs (i.e., exciton BEC and e-h BCS state) is not allowed. The calculation is performed at absolute zero temperature.

* Corresponding author. Tel.: +81-6-6850-5735; fax: +81-6-6850-5351

Email address: tomio@acty.phys.sci.osaka-u.ac.jp (Yuh Tomio).

2. Two-site dynamical mean-field theory

We consider a electron-hole system described by the two-band Hubbard model given by

$$H = - \sum_{\langle ij \rangle > \sigma} \sum_{\alpha=e,h} t_{\alpha} d_{i\sigma}^{\alpha\dagger} d_{j\sigma}^{\alpha} - \sum_{i\sigma,\alpha} \mu_{\alpha} d_{i\sigma}^{\alpha\dagger} d_{i\sigma}^{\alpha} + U \sum_{i,\alpha} d_{i\uparrow}^{\alpha\dagger} d_{i\uparrow}^{\alpha} d_{i\downarrow}^{\alpha\dagger} d_{i\downarrow}^{\alpha} - U' \sum_{i\sigma\sigma'} d_{i\sigma}^{e\dagger} d_{i\sigma}^e d_{i\sigma'}^{h\dagger} d_{i\sigma'}^h, \quad (1)$$

where $d_{i\sigma}^{\alpha\dagger}$ ($d_{i\sigma}^{h\dagger}$) denotes a creation operator of a conduction band electron (a valence band hole) with spin $\sigma = \{\uparrow, \downarrow\}$ at the i -th site. The quantities t_e (t_h) and μ_e (μ_h) are the transfer integral of the electrons (holes) between the neighboring sites and the chemical potential measured from the center of the electron (hole) band, respectively. The on-site Coulomb interaction of the e-e (h-h) repulsion and that of the e-h attraction are expressed by U and $-U'$, respectively. The local Green function for electrons or holes of the model (1) is defined by

$$G^{\alpha}(\omega) = \langle\langle d_{i\sigma}^{\alpha}; d_{i\sigma}^{\alpha\dagger} \rangle\rangle_{\omega} = \int_{-\infty}^{\infty} d\varepsilon \frac{\rho_0^{\alpha}(\varepsilon)}{\omega + \mu_{\alpha} - \varepsilon - \Sigma^{\alpha}(\omega)}, \quad (2)$$

where $\Sigma^{\alpha}(\omega)$ is the self-energy of electrons ($\alpha = e$) or holes ($\alpha = h$), which is local, i.e., does not depend on the wave number, in the limit of infinite-dimensions. We use the semicircular density of states (DOS), $\rho_0^{\alpha}(\varepsilon) = \sqrt{4t_{\alpha}^2 - \varepsilon^2}/(2\pi t_{\alpha}^2)$.

Within the DMFT [2], the many-body problem of the lattice model (1) is mapped onto the problem of a single-site impurity embedded in an effective medium. The effective medium, which is dynamical and is represented by the noninteracting impurity Green function $\mathcal{G}_0^{\alpha}(\omega)$ of an effective single-impurity Anderson model (SIAM), is determined from the self-consistency condition $\mathcal{G}_0^{\alpha}(\omega)^{-1} = \omega + \mu_{\alpha} - t_{\alpha}^2 G^{\alpha}(\omega)$. The condition is also read as $G_{\text{imp}}^{\alpha}(\omega) = G^{\alpha}(\omega)$. The interacting impurity Green function of the effective SIAM, $G_{\text{imp}}^{\alpha}(\omega)$, should be calculated exactly such that effects of the interactions on the impurity site are fully included. Contrary to the ordinary mean-field approaches, thus, in the DMFT scheme the local correlations and dynamical quantum fluctuations are taken into full account.

In order to extract a sketch of the phase diagram of the model (1), here we apply the two-site DMFT [3] which is simplified version of the DMFT. In the two-site DMFT, the effective medium $\mathcal{G}_0^{\alpha}(\omega)$ is represented approximately by only the fewest parameters, i.e., the effective SIAM consists of a single impurity and only a single bath sites. Since the essence of the DMFT concerning the local correlations still remains despite the bold approximation and simplification, it can be successful to provide the most correct critical point

of the Mott-Hubbard transition and to describe the qualitative electronic properties [3].

For the model (1), the corresponding effective two-site SIAM is written as

$$H_{\text{imp}} = \sum_{\sigma,\alpha} \left[\varepsilon_c^{\alpha} c_{\sigma}^{\alpha\dagger} c_{\sigma}^{\alpha} + V_{\alpha} \left(d_{\sigma}^{\alpha\dagger} c_{\sigma}^{\alpha} + \text{h.c.} \right) - \mu_{\alpha} d_{\sigma}^{\alpha\dagger} d_{\sigma}^{\alpha} \right] + U \sum_{\alpha} d_{\uparrow}^{\alpha\dagger} d_{\uparrow}^{\alpha} d_{\downarrow}^{\alpha\dagger} d_{\downarrow}^{\alpha} - U' \sum_{\sigma\sigma'} d_{\sigma}^{e\dagger} d_{\sigma}^e d_{\sigma'}^{h\dagger} d_{\sigma'}^h, \quad (3)$$

where the bath parameters V_{α} and ε_c^{α} denote the hybridization between the impurity (d) and bath (c) sites, and the energy level of the bath site, respectively. The Green function of the effective medium (i.e., noninteracting impurity Green function) becomes $\mathcal{G}_0^{\alpha}(\omega)^{-1} = \omega + \mu_{\alpha} - V_{\alpha}^2/(\omega - \varepsilon_c^{\alpha})$. In the two-site DMFT, the self-consistency condition is reduced to simpler equation by the following procedure [3]: the self-energy is expanded in the low-energy region, $\Sigma^{\alpha}(\omega) \sim a_{\alpha} + b_{\alpha}\omega$, and then the resulting local Green function (2) and impurity Green function $G_{\text{imp}}^{\alpha}(\omega)^{-1} = \mathcal{G}_0^{\alpha}(\omega)^{-1} - \Sigma^{\alpha}(\omega)$ are compared so as to coincide at high-energy region. Thereby, the self-consistency equation for V_{α} is obtained as

$$V_{\alpha}^2 = t_{\alpha}^2 Z_{\alpha}, \quad (4)$$

where

$$Z_{\alpha} = (1 - b_{\alpha})^{-1} = \left[1 - \frac{d\Sigma^{\alpha}(\omega)}{d\omega} \Big|_{\omega=0} \right]^{-1}, \quad (5)$$

is the quasiparticle weight which generally characterizes the Fermi liquid (metallic) states. On the other hand, the requirement that the particle densities of the original and impurity models must be equal, i.e., $n^{\alpha} = n_{\text{imp}}^{\alpha}$, leads to the self-consistency condition for ε_c^{α} ,

$$\int_{-\infty}^0 d\omega \text{Im} G^{\alpha}(\omega + i0^+) = \int_{-\infty}^0 d\omega \text{Im} G_{\text{imp}}^{\alpha}(\omega + i0^+). \quad (6)$$

Consequently, the model (1) can be solved within the two-site DMFT by the following self-consistency cycle: (i) $G_{\text{imp}}^{\alpha}(\omega)$ is directly calculated by the exact diagonalization of the two-site SIAM (3) with ε_c^{α} and V_{α} . (ii) By using $\Sigma^{\alpha}(\omega) = \mathcal{G}_0^{\alpha}(\omega)^{-1} - G_{\text{imp}}^{\alpha}(\omega)^{-1}$, a new value of V_{α} is determined from the condition (4) and Eq. (5). (iii) By substituting $\Sigma^{\alpha}(\omega)$ for Eq. (2), a new value of ε_c^{α} is chosen so as to satisfy the condition (6). This process (i)-(iii) is iterated until ε_c^{α} and V_{α} converge.

The metal-insulator transition for the normal phase of the model (1) is discussed from behaviors of both the quasiparticle weight Z_{α} and the interacting DOS $\rho^{\alpha}(\omega) = -\text{Im} G^{\alpha}(\omega + i0^+)/\pi$, with varying $U, U', t_h/t_e$ and also the particle density n ($\equiv n^e = n^h$).

3. Phase diagram at half filling

First, we concentrate on the special case where the both electron and hole bands are half-filled, i.e., $n = 1$. In this symmetric case, we can set $\mu_\alpha = U/2 - U'$ and $\varepsilon_c^\alpha = 0$.

For $t_h/t_e = 1$ (the mass of the hole is the same as that of the electron), the phase diagram on the plane of U' and U is shown in Fig. 1. There are three kinds of states: (I) metallic state, (II) Mott-Hubbard insulating state, and (III) biexciton-like insulating state. The second-order transitions between these states occur on the solid curves. In the metallic state (I), Z_α has a finite value and there is finite DOS at the Fermi level (the quasiparticle coherent peak), i.e., $\rho^\alpha(0) \neq 0$. On the other hand, in the both insulating states (II) and (III), $Z_\alpha = 0$ and the coherent peak of the DOS disappears. However, the physical pictures of the insulating states (II) and (III) are quite different, as drawn schematically in Fig. 1: the state (II) is induced by the e-e (h-h) repulsion U on each electron and hole band, while the state (III) is realized by the e-h attraction U' on each site. The competition of these two states stabilizes the metallic state for $U \simeq U'$.

We point out that the above results are equivalent to those obtained for the two-orbital repulsive Hubbard model [4] because this model and our model (1) only at half-filling can be mapped onto each other by the attraction-repulsion transformation. Actually, the phase diagram of Fig. 1 is in good agreement with that of Ref. [4].

We also examine effects of the difference between the electron and hole masses. In Fig. 2, the phase diagram on the plane of U' and U is shown for $t_h/t_e = 0.5$, where the hole is twice as heavy as the electron. A new state (IV) appears between states (I) and (II), in which $Z_e \neq 0$ but $Z_h = 0$, i.e., the electron (hole) band is metallic (insulating). In other words, the Mott-Hubbard transition of holes does not coincide with that of electrons

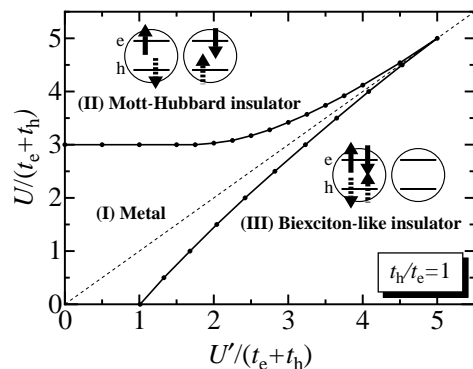


Fig. 1. Phase diagram in the U' - U plane at half-filling ($n = 1$) for $t_h/t_e = 1$.

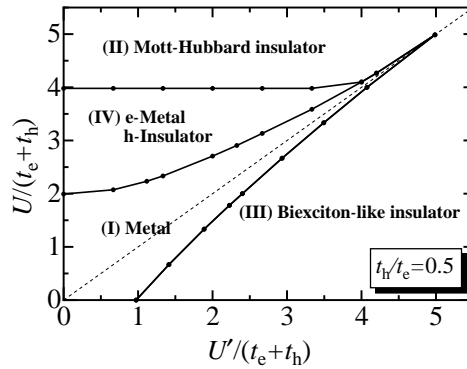


Fig. 2. Phase diagram in the U' - U plane at half-filling ($n = 1$) for $t_h/t_e = 0.5$.

when $t_e \neq t_h$. This “band-selective” Mott-Hubbard transition corresponds to the “orbital-selective” Mott transition in the two-orbital repulsive model [5]. But more than the above, what we should emphasize here from common features of Figs. 1 and 2 is as follows. (i) The metal-insulator transition between states (I) and (III) is by no means “band-selective” for any ratio t_h/t_e . (ii) The position of that phase boundary on the plane of interactions scaled by $t_e + t_h$ is universal with regard to the ratio t_h/t_e . These facts indicate that the transition between the metallic state (I) and the biexciton-like insulator (III) occurs as a result of the competition between the interactions and the relative motion of electron and hole. Note that the quantity $t_e + t_h$ is proportional to the energy of the relative motion.

4. Phase diagram at arbitrary filling

In this section, we discuss the case of arbitrary filling. For $n \neq 1$, the process for determining of the chemical potential μ_α is added to the self-consistency cycle for ε_c^α and V_α . Hereafter $t_h/t_e = 1$ is fixed.

Fig. 3 shows the phase diagram on the plane of U' and U for $n = 0.8$. The Mott-Hubbard insulator (II) disappears immediately away from half-filling, as known in the single-band Hubbard model [2,3], while the metallic state (I) and the biexciton-like insulator (III) remain. In the present two-site DMFT calculation, only the metallic state in which both Z_α and $\rho^\alpha(0)$ are nonzeros, is always obtained for $U > U'$ within the present parameter region. However, it seems to express a limitation of the two-site DMFT and the consideration in the limit of $U \rightarrow \infty$ actually leads the following results.

In the limit of $U \rightarrow \infty$, the model (1) can be mapped onto a single-band attractive Hubbard model with the attraction $-U'$. From the results of the DMFT study

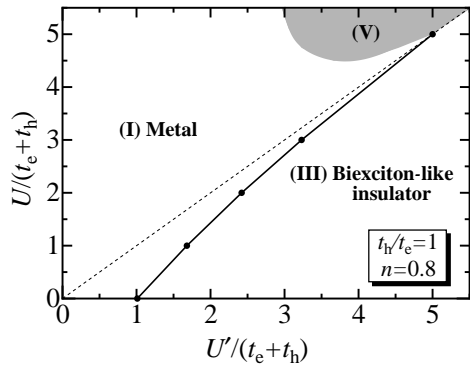


Fig. 3. Phase diagram in the U' - U plane for $t_h/t_e = 1$ and $n = 0.8$. The shaded area indicates the region speculated that the exciton-like insulator (local e-h pairing state) appears.

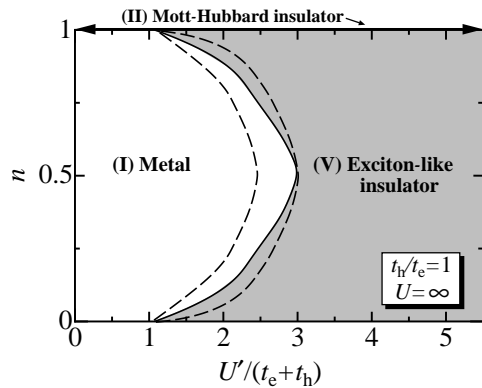


Fig. 4. Phase diagram in the U' - n plane with $t_h/t_e = 1$ for the limiting case of large U , referred from Ref. [7]. The interval area between two dashed curves is the coexistent region of the metallic and exciton-like insulating states.

of this model [6,7], then, we can draw the phase diagram on the plane of U' and n in the limit of $U \rightarrow \infty$, as shown in Fig. 4. In addition to the metallic state (I) and the Mott-Hubbard insulator (II) (just on $n = 1$ for all values of U'), the exciton-like insulating state (V) appears, in which the incoherent local e-h pairs (do not condense) are formed. It is worthy to note that the transition between the metallic (I) and exciton-like insulating (V) states is the first-order transition (except for $n = 0, 0.5$ and 1). As well as has been argued in Refs. [6,7], the exciton-like insulator (V) will be characterized by that $Z_\alpha \neq 0$ but $\rho^\alpha(0) = 0$ (i.e., a gap opens at Fermi level), however which cannot be described within the two-site DMFT since the gap formation ($V_\alpha = 0$) is directly connected to $Z_\alpha = 0$ through Eq. (4) in the present scheme.

Let us now return to Fig 3. Based on both the result of Fig. 4 and the behavior of Z_α in the metallic state, it could be surmised that the exciton-like insulator appears around the shaded region of Fig. 3, in which U' is comparatively large and Z_α of the metallic solution is

quite small. To describe the exciton-like insulator and determine that phase boundary for the finite U are left for the future work.

5. Discussions

In this paper, we found the phase transitions among the exciton-like insulator, biexciton-like insulator, and the metallic state, for arbitrary filling with the use of the DMFT. This implies that the exciton Mott transition can be described essentially in terms of the simple lattice model with only short-range interactions as well as the Mott-Hubbard transition.

Finally, we discuss the relevance of our assumption that the e-h pairs do not condense. Although the calculation was performed at zero temperature, we believe that our present results will be valid for the intermediate temperatures, i.e., above critical temperature (T_C) of exciton BEC, but below temperature corresponding to the e-h binding energy (E_B). From simple evaluation of T_C and E_B , it can be shown that such a temperature region actually exists: consider again in the limit of $U \rightarrow \infty$. In the strong limit of U' , T_C can be estimated as of order $(t_e + t_h)^2/U'$ [8,9]. On the other hand, in the low-density limit $n \rightarrow 0$, E_B can be estimated as of order U' [9]. Comparing these two characteristic temperatures, it can be concluded that such an intermediate temperature region exists even for not so large U' ($\sim t_e + t_h$). Of course, the temperature effect and the problem of condensation will be investigated by more precise calculation.

This work is supported by CREST, JST.

References

- [1] See, for example, S. A. Moskalenko, D. W. Snoke, Bose-Einstein Condensation of Excitons and Biexcitons, Cambridge Univ. Press 2000.
- [2] For a review, see A. Georges, G. Kotliar, W. Krauth, M. J. Rozenberg, Rev. Mod. Phys. 68 (1996) 13.
- [3] M. Potthoff, Phys. Rev. B 64 (2001) 165114.
- [4] A. Koga, Y. Imai, N. Kawakami, Phys. Rev. B 66 (2002) 165107.
- [5] A. Koga, N. Kawakami, T. M. Rice, M. Sgrist, Phys. Rev. Lett. 92 (2004) 216402.
- [6] M. Keller, W. Metzner, U. Schollwöck, J. Low Temp. Phys. 126 (2002) 961.
- [7] M. Capone, C. Castellani, M. Grilli, Phys. Rev. Lett. 88 (2002) 126403.
- [8] P. Nozières, S. Schmitt-Rink, J. Low Temp. Phys. 59 (1985) 195.
- [9] R. Micnas, J. Ranninger, S. Robaszkiewicz, Rev. Mod. Phys. 62 (1990) 113.